Encoded Hydrogel Microparticles for Sensitive and Multiplex microRNA Detection Directly from Raw Cell Lysates

analytical chemistry

Article

pubs.acs.org/ac

Encoded Hydrogel Microparticles for Sensitive and Multiplex microRNA Detection Directly from Raw Cell Lysates

Hyewon Lee,[†,‡] Sarah J. Shapiro,[†] Stephen C. Chapin,[†] and Patrick S. Doyle*[,†]

[†]Department of Chemical Engineering, Massachusetts Institute of Technology, Cambridge, Massachusetts 02139, United States

[‡]Synthetic Biology & Bioengineering Research Center, Korea Research Institute of Bioscience & Biotechnology (KRIBB), Daejeon 34141, South Korea

Supporting Information

ABSTRACT: In recent years, microRNAs (miRNAs) have emerged as promising diagnostic markers because of their unique dysregulation patterns under various disease conditions and high stability in biological fluids. However, current methods of analyzing miRNA levels typically require RNA isolation, which is cumbersome and time-consuming. To achieve high-throughput and accurate miRNA profiling, this study eliminates the need for purification steps by detecting miRNA directly from raw cellular lysate using nonfouling polyethylene glycol microparticles. In contrast to recent studies on direct miRNA measurements from cell lysate, our hydrogel-based system provides high-confidence quantification with robust performance. The lysis buffer for the assay was optimized to maximize reaction and labeling efficiency, and this assay has a low limit of detection (<1000 cells) without target amplification. Additionally, the capability for multiplexing was demonstrated through analyzing the levels of three endogenous miRNAs in 3T3 cell lysate. This versatile platform holds great potential for rapid and reliable direct miRNA quantification in complex media, and can be further extended to single-cell analysis by exploiting the flexibility and scalability of our system.

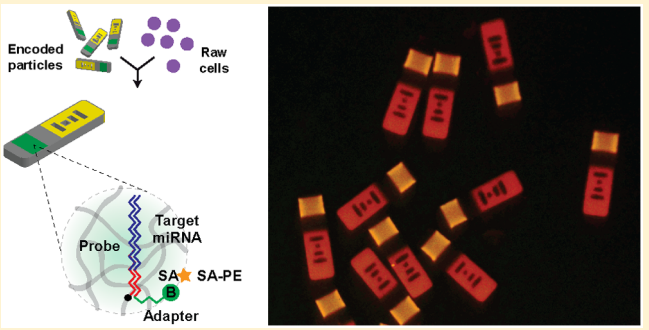

MicroRNAs (miRNAs) are a class of small noncoding RNAs that play significant roles in the post-transcriptional regulation of gene expression and diverse cellular functions. It has been shown that many diseases including a variety of cancers,[1−3] psychiatric syndromes,[4] diabetes,[5] and cardiovascular diseases[6,7] correlate to dysregulation of these small RNAs. With a high value, miRNAs have gained increasing popularity as potential novel biomarkers in disease diagnosis and prognosis.[8] Despite their great promise, the quantification of miRNAs is practically challenging due to their unique properties such as small size, high levels of sequence homology, and wide range in abundance.[8−10] While the existing approaches including quantitative real-time polymerase chain reaction (qRT-PCR), microarray, and deep sequencing have high sensitivity, they are costly, inconsistent, and do not address all crucial clinical needs.[8,9,11] Moreover, PCR-based systems require great care with primer design due to their target-based amplification, and often introduce sequence bias.[9,12] Microarrays, however, allow large-scale parallel detection of miRNAs, but usually require relatively long assay times with complicated steps.[9,13] Therefore, there is a great demand for systems that provide high sensitivity and specificity without target-based amplification, a simple workflow, and the ability to multiplex small panels of miRNAs in a high throughput manner.

In addition, sample processing and RNA extraction is also crucially important for reliable miRNA quantification. A large fraction of miRNAs is associated with protein complexes as a mechanism for their stability, and located within cells.[8] Due to this high stability, miRNAs present a promising target for diagnostics, yet require efficient and careful cell lysis to recover intact target molecules for capture to complementary probes. Also, to remove undesirable entities for either maintaining the activity of an enzyme like polymerase or reducing fouling, most existing technologies require additional total RNA isolation prior to running a miRNA assay.[14−17] However, RNA extraction is technically challenging and typically rate-limiting. Recent development of commercial and in-house reagents has enabled the simple preparation of crude cell lysates suitable for direct miRNA measurement.[18−20] While advantageous in assay throughput, these reagents typically generate large variations in miRNA quantification, decreasing assay reliability. Moreover, commercial buffers are often costly and less informative in buffer components, limiting assay flexibility. In a different manner, Ryoo et al. has demonstrated the development of biosensors to quantify miRNA expression levels in living cells.[21] However, this approach requires long assay times (14 h) and provides low sensitivity (1 pM). Thus, rapid and reliable direct

Received: October 15, 2015
Accepted: February 10, 2016

DOI: 10.1021/acs.analchem.5b03902
Anal. Chem. XXXX, XXX, XXX−XXX

measurement of miRNAs from crude cellular lysate has become of great interest in disease diagnosis.

To overcome these limitations, we sought to use polyethylene glycol (PEG) hydrogel particles. In previous work, we demonstrated the superiority of nonfouling PEG hydrogels for the detection of biomolecules such as DNA, proteins, and miRNA in complex media.[22−26] In addition, a hydrogel substrate provides an aqueous reaction environment, which leads to more favorable association of targets than surface-based sensing platforms.[26−28] Also, a 3-dimensional gel matrix offers high and uniform loading capacity of probe molecules, and reduces the energy barrier for access to target probes with less steric hindrance. We use a novel high-throughput stop-flow lithography (SFL) technique to simultaneously synthesize gel particles in microfluidic devices with highly reproducible compositions.[29,30] After a single polymerization step, particles bear spatially distinct regions of code and probe. The fluorescently doped code region consists of a series of unpolymerized holes to identify the specific DNA probe functionalized for miRNA target capture. Our encoding scheme allows multiplexed analysis and its capacity can be easily augmented to millions by adding more holes. With these particles, we previously demonstrated rapid miRNA detection with atto-mole sensitivity by employing a unique ligation-based labeling scheme after hybridization.[22] This posthybridization scheme is very efficient and uses the same adapter regardless of the miRNA target, which eliminates the possibility of sequence-bias.

In this paper, we demonstrate the multiplexed quantification of endogenous miRNAs on barcoded hydrogel particles directly from raw cells without the need for RNA extraction in a 2 h and 45 min assay. By using an optimized buffer system, it is possible to liberate miRNAs from cells and carrier proteins for highly efficient capture of miRNA targets. To fluorescently label bound miRNA targets without the risk of sequence bias, we adopt the unique post target-hybridization labeling scheme. The assay provides high sensitivity with a limit of detection of hundreds of individual cells without target amplification over a three log range while allowing multiplexing across at least three endogenous targets.

Moreover, this detection platform is a highly tunable and scalable analysis system. It has been known that miRNA copy numbers are highly variable over 4 orders of magnitude in a given cell, depending on cell type and state.[8] Also, cell-to-cell expression is often heterogeneous, requiring large-scale analysis for the quantification of multiple miRNA expressions at the single-cell level. To translate to a single assay, one often relies on sequence-dependent target amplification via RT-PCR,[31,32] which potentially requires probe-set modification that may be difficult to scale-up. Instead, our versatile system is capable of incorporating a signal-based amplification scheme[23,33−35] such as rolling circle amplification (RCA) without a need for extensive optimization regardless of cell type or miRNA target. This sensitivity can be improved further (over 2 orders of magnitude) by running the assay in nanoliter chambers. We anticipate that the results presented here will allow rapid and reliable clinical profiling of miRNAs, which can potentially be extended to single cell analysis.

EXPERIMENTAL SECTION

Particle Synthesis. Hydrogel particles were synthesized using stop flow lithography.[29,30] Briefly, 250 μm by 70 μm hydrogel particles were formed by coflowing streams of monomer through a polydimethylsiloxane (PDMS) device. The flow was paused, and UV light was transmitted through a mask positioned in the field stop of the microscope to cross-link the monomer and form particles. The hydrogel particles used in this study contained four regions: a code region containing rhodamine with holes for particle identification, a probe region containing an acrylate modified miRNA probe, cross-linked into the hydrogel, and two spacer regions, which flanked the probe region to unify the mass transport resistance on both ends and isolate it from the fluorescence of the code region. The monomer solutions were composed of polyethylene glycol diacrylate (PEG-DA) monomer with 200 MW PEG used as a porogen to increase diffusion through the particles. The code and spacer regions were formed from a 35% v/v PEG-DA solution diluted 9:1 with either rhodamine or color dye for visualization. The probe region consisted of a 20% v/v PEG-DA solution diluted 9:1 with the probe. The probe concentration was adjusted based on the relative binding rate as described previously,[22] resulting in concentrations of 247 μM for miR-21, 50 μM for miR-145, and 111 μM for miR-146a.

Assay Protocol. The synthesized particles were used in a bioassay to analyze concentrations of miRNA in cell lysate. For maximum sensitivity and reliable measurement of miRNA, we have used ∼50 particles in each incubation tube for all incubations. All reaction steps were conducted in a thermoshaker (MultiTherm Shaker, Thomas Scientific) at 1500 rpm. Cells were rinsed in PBS with 0.1% BSA three times prior to beginning the assay. In the first assay step, the cells were lysed and the target miRNA was simultaneously hybridized to the hydrogel-linked complementary probe. The previous study reported that the small size of the RNA target (∼20bp) allows it to completely penetrate all regions of the particle, hybridizing throughout the incubation period.[26] This hybridization step was conducted for 90 min at 55 °C in 1X Tris-EDTA buffer with 0.05% Tween-20 (1X TET) containing 350 mM NaCl, 2% (w/v) sodium dodecyl sulfate (SDS) and 200 μg/mL proteinase K in a total reaction volume of 50 μL. The SDS served as a lysing agent, while the proteinase K degraded associated proteins to release miRNAs for capture. Following miRNA capture, samples were rinsed three times with washing buffer (50 mM NaCl in TET). In each rinse step, we added 500 μL of washing buffer to the incubation tube. After vortexing and centrifugation, all but 50 μL of solution was aspirated from the incubation tube through manual pipetting. Next, the biotinylated universal linker sequence hybridized to the portion of the probe specific for the universal linker and was ligated to the miRNA. This step was conducted in buffer containing ATP, the universal linker, and T4 DNA ligase for 30 min at 21.5 °C. The exact buffer composition is listed in Table S3. Following the ligation of the linker, the solution was rinsed three times with washing buffer. For signal, samples were incubated with 1.8 μg/mL streptavidin conjugated R-phycoerythrin (Life Technologies) in 1X TET buffer containing 50 mM NaCl. After another three-rinse cycle, the streptavidin−biotin bond resulted in fluorescence in the probe region, proportional to the amount of hybridized miRNA, which was visualized by applying light at the PE excitation wavelength using a filter set from Omega Optical (filter set XF101−2). The particles were imaged on a Zeiss Axio Observer A1 microscope using a 20X objective, an Andor Clara CCD camera and Andor SOLIS software.

Assay from Freeze−Thaw Cell Lysate. To investigate the compatibility with freeze−thaw cell lysate, cell lysate was

DOI: 10.1021/acs.analchem.5b03902
Anal. Chem. XXXX, XXX, XXX−XXX

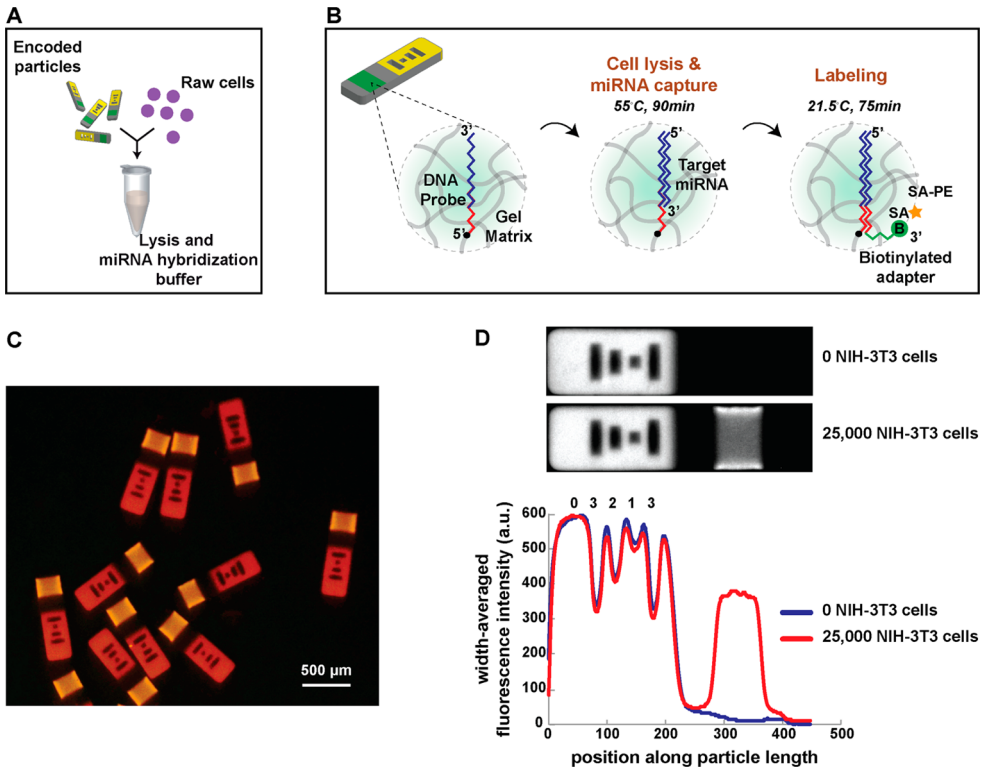

Figure 1. (A) For direct miRNA measurement from raw cells, hydrogel particles and cells are incubated with buffer in a one-step lysis and hybridization. (B) Schematic illustrating the assay workflow. In the first assay step, cells are lysed, and the target miRNA hybridizes to the complementary probe at 55 °C for 90 min. During labeling at 21.5 °C for a total of 75 min, a biotinylated universal linker binds to the probe and is ligated to the miRNA. R-phycoerythrin conjugated streptavidin then binds to the biotin generating fluorescence within the probe region. (C) Fluorescent image of particles after complete assay, illustrating the consistency of target binding and labeling in probe region. The rhodamine-containing code regions are also easily distinguishable. (D) Scan represents incubation with 0 (blue) or 25 000 3T3 cells (red) with corresponding fluorescent images of particles with code 03213 on top.

prepared prior to running the assay. The cells at desired concentration (here, 100 000 cells/μL) were lysed by 90 min incubation at 55 °C in 1X TE buffer with 0.5% Tween-20 (v/v) with 2% (w/v) SDS and 200 μg/mL PK. Then, the lysate was frozen at −20 °C in 100 μL aliquots. For the miRNA assay, frozen lysate was thawed at room temperature, and sequentially, hybridization and labeling were performed as described in the above section and previous papers.[22,23,35]

Data Analysis. After each particle was imaged, the image was aligned and cropped using ImageJ[36] (National Institutes of Health), and the total fluorescence intensity from the probe region was averaged to calculate the total fluorescence using a custom MATLAB script. The background fluorescence was calculated by averaging the fluorescence in a region outside of the particle and was subtracted from the probe fluorescence to generate background-subtracted signals. The net signal was then found by subtracting the background-subtracted signal of the control particle from the background subtracted signal of the particle of interest. For all studies, 4−8 particles were analyzed to compute average fluorescence intensities.

Determination of Limit of Detection (LOD). The limit of detection was determined according to previously published protocols.[35] The noise of the measurement was defined to be the standard deviation of the control probe signal, after incubation with 0 cells or 0 amol of synthetic targets. Then, the limit of detection was defined to be the cellular concentration at which the net signal-to-noise ratio was equal to 3. This was calculated by plotting the signal-to-noise ratio vs either the cellular concentration or the amount of synthetic miRNA (also, see Figure S3). The data points were fit to a line, and the line was extrapolated to find the cellular concentration or synthetic miRNA amount at which the net signal was equal to three times the control probe fluorescence (signal-to-noise ratio of 3). This cell concentration is the limit of detection of the assay.

RESULTS AND DISCUSSION

Assay Optimization. We sought to apply our PEG hydrogel microparticles to measure the endogenous miRNA expressions in crude cell lysate without a total RNA extraction procedure. It is previously reported that such PEG-based particles prevent nonspecific binding and enable the direct detection of biological molecules in complex media due to the nonfouling and biofriendly nature of the scaffold.[22−26] With the synthesized encoded gel microparticles, we directly added raw 3T3 cells to the reaction tube and modified our assay protocol as described in the Experimental Section (Figure 1A). To release cellular content including miRNAs, the tube contained detergent (SDS) and proteinase K (PK) in addition to hybridization buffer to disrupt bonds within cell walls and denature proteins possibly associated with miRNAs. Under our optimized hybridization buffer conditions, only the target miRNAs bind to the complementary probe functionalized in the hydrogel particles (Figure 1B). Then, we employed a two-step labeling method with biotinylated universal linker and phycoerythrin-conjugated streptavidin reporter (SA-PE). In an initial trial with a spike of 500 amol of synthetic miRNAs, we observed specific and consistent fluorescent signals on the probe region of the particles (Figure 1C). Importantly, this

DOI: 10.1021/acs.analchem.5b03902
Anal. Chem. XXXX, XXX, XXX−XXX

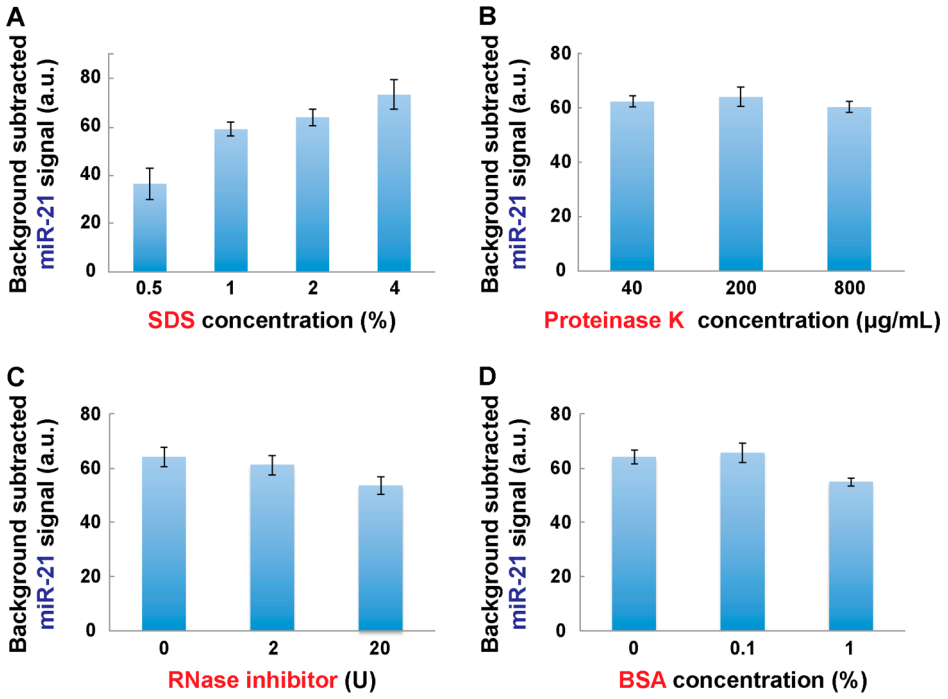

Figure 2. Optimization of the lysis buffer conditions regarding (A) sodium dodecyl sulfate (SDS), (B) Proteinase K, (C) RNase inhibitor, and (D) bovine serum albumin (BSA). In all cases, NIH-3T3 cell concentration is 100 cells/μL. Error bars represent standard deviation (n = 4–7).

universal linker in our labeling scheme is used for every single gel regardless of the intended miRNA target, which eliminates the possibility of sequence-bias and provides high flexibility in the choice of the reporter molecules.

To evaluate the compatibility of crude cell lysate with the particles, we first tested the endogenous expression of miR-21, which has been known to be involved in various cellular functions. Preliminary tests with miR-21-specific particles with code 03213 showed that our assay scheme provided measurable signal from ~250 000 3T3 cells without any significant adsorption on nonprobe regions of the particles (Figure 1D). This nonfouling property enables not only accurate quantification of target miRNAs but also rapid decoding of our barcode particles, which is critical in a multiplex assay. Thus, this experimental result suggests that our assay platform and protocol are feasible for the direct detection of multiple miRNAs from raw cells.

For the efficient recovery of miRNAs to achieve sensitive measurement, we further optimized the cell lysis conditions. Strong ionic detergents such as SDS are one of the most widely used cell-lysis techniques for biochemical assays, since they provide fast cell lysis on the order of seconds without the need for specialized equipment.[37] For optimization, we analyzed the impact of combining the hybridization buffer with detergent, protease, and RNase inhibitor. In all assays, we analyzed the endogenous miR-21 signals from 5000 3T3 cells. It is important to note that control signals from different buffer conditions exhibited negligible differences (Figure S1). As shown in Figure 2A, target capture increased as the concentration of SDS was raised from 0.5 to 4% (w/v) at constant PK (200 μg/mL). Above 4% SDS, the fluorescent signal decreased (data not shown). By considering both signal intensity and variability, we proceeded using 2% (w/v) SDS. Next, we evaluated the effects of PK, which was introduced to denature carrier proteins of miRNAs. Also, it has been known that PK efficiently digests and inactivates RNase and DNase in the presence of SDS.[38] There were not significant differences in fluorescence among three different concentrations of PK at 2% (w/v) SDS, but 200 μg/mL PK resulted in the highest target signal (Figure 2B). To determine whether adding RNase inhibitor would increase the fluorescent signal, 0, 0.2, or 20 U of RNase inhibitor were added to the reaction (0, 4, and 400 U/mL in final reaction volume, respectively). However, we observed that the sample without RNase inhibitor had a higher fluorescent signal (Figure 2C), likely due to the absence of the glycerol-based buffer in which the RNase inhibitor was stored. Furthermore, to explore the effect of a blocking agent during lysis/capture, we added BSA to the reaction buffer. This test resulted in lower signals for 0.1% and 1% (w/v) BSA than preparations without BSA in the reaction mixture (Figure 2D), indicating that a blocking agent is not required for this assay, presumably due to the nonfouling nature of the gel particles. Actually, it was postulated that adding high BSA possibly hinders the transfer of target molecules. Importantly, the solution used to wash the cells prior to the lysis/hybridization step is required to include BSA (normally at 0.1% (w/v)) to prevent cell loss on tube and tip surfaces. On the basis of the optimization results, we decided to use 2% (w/v) SDS and 200 μg/mL PK in subsequent studies to maximize the target capture.

Detection Performance. Using the protocol optimized here, we investigated the effect of lysis buffer components on target-probe binding and labeling efficiency with 500 amol of synthetic miR-21. As shown in Figure 3, SDS and PK induced only a small decrease (~1.2%) of miR-21 signal intensity. Also, Figure S2 demonstrates that the optimized lysis buffers provided repeatable results from two separate measurements. This high performance and reproducibility of the assay implies that the buffer complexity did not affect assay performance, which requires no further modification in ensuing assays. Also, this indicates that the lysis buffer components did not impair the function of the T4 DNA ligase used during the labeling step, suggesting that the rinse steps effectively removed the

DOI: 10.1021/acs.analchem.5b03902
Anal. Chem. XXXX, XXX, XXX–XXX

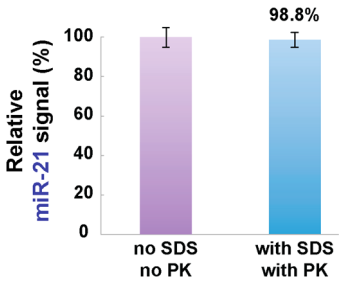

Figure 3. Assay validation. Comparison of the fluorescent miR-21 signal with and without dodecyl sodium sulfate (SDS) and Proteinase K (PK). Fluorescence values are normalized as a percentage of the net miR-21 signal of the samples without SDS or PK. Error bars represent standard deviation (n = 4–5).

SDS and PK from the hydrogels after cell lysis/target binding. Moreover, to validate the accuracy of our assay scheme, we compared this fluorescent signal from 500 amol spikes of synthetic target in 2% SDS and 200 μg/mL PK to the endogenous miR-21 signal previously measured from 5000 3T3 cells in the same buffer. The fluorescent signal from 5000 3T3 cells was similar to ~71.4 amol synthetic miR-21, allowing us to approximate the copy number as ~8600 copies of miR-21 per 3T3 cell. This correlates well with a previously published estimate of ~8327 copies per 3T3 cell obtained using Northern blots.[17]

Next, we examined the assay sensitivity and dynamic range for synthetic and endogenous miR-21 by plotting calibration curves. In each reaction tube containing lysis/miRNA capture buffer, we incubated either synthetic miRNA spikes (from 2.5 amol to 5 fmol) or crude cell lysates (from 1000 to 500 000 3T3 cells). As shown in Figure 4, our assay scheme provided an excellent linear response over ~3 logs for both synthetic and endogenous targets with $R^2 \approx 0.99$. From the calibration curve, we calculated the limit of detection (LOD) based on the analysis our group has previously conducted (see the Experimental Section for details).[22,23,35] To determine the LOD, a plot of the signal-to-noise ratio (SNR) as a function of concentration was fit with a line and extrapolated to find the concentration at which the SNR equals three, which was defined to be the assay LOD (Figure S3). Importantly, this SNR was derived from the net signal by subtracting the control signal (obtained with the 0 amol spike-ins or 0 cells) from the target signal so that the assay background was accounted for in the analysis. The assay from synthetic spikes demonstrated a LOD of 2.4 amol, which is comparable to the previous studies that were validated with qRT-PCR.[22] This indicates that the lysis buffer does not affect the assay performance. In the case of 3T3 cell lysate, we determined that endogenous miR-21 quantification can be accomplished with as few as ~857 cells. Previously, Ho et al. has reported microRNA LODs of 200 cells,[19] which is within an order of magnitude of the LOD obtained with our hydrogel-based detection. Even though some recent studies on direct miRNA measurements demonstrate high sensitivity (1–1000 cells),[18,20] their measurements are based on target-based amplification of qRT-PCR. This target-based amplification often introduces sequence bias. In future, our highly flexible synthesis and assay scheme can be readily integrated with locked nucleic acid (LNA) probes and/or a signal-based amplification scheme with the use of multiple fluorophores to improve system sensitivity.

Furthermore, we noted that a mean intratrial CV of 8–9% was calculated for both endogenous and synthetic miRNA targets. This was in contrast to other methods for direct quantification of miRNA from crude cell lysates, which showed typically high variations (CV 12.7%–47.8%).[19] It is importantly noted that our small CV represents the high quality of RNA recovery from raw cells with our lysis buffer and high accuracy in miRNA measurement with a hydrogel-based detection platform. Thus, we need only a small number of particles (<~10 particles) for reliable analysis, which is beneficial for high-throughput assays.

Additionally, we examined the freeze–thaw performance using cell lysates (25 000 3T3 cells) prepared from our lysis buffer (2% SDS and 200 μg/mL PK). Generally, it has been shown that miRNAs are highly stable in cell lysates and can be stored at −20 and/or −80 °C for days.[18,19] In our proof-of-concept test of freeze–thaw cell lysate, the endogenous miR-21 signal was decreased by ~50% compared to fresh cell lysates (Figure S4). This signal decrease is probably due to freeze/thaw temperatures (here, −20 °C/room temperature) or absence of RNase inhibitor; a previous study demonstrated that RNA stability was enhanced when stored at −80 °C or thawed at 4 °C or RNase inhibitor added.[18] For better assay reliability and sensitivity, it is possible to further optimize our assay protocol in the future.

Multiplex Detection. Our next task was to evaluate the multiplex performance in crude cell lysate. It has been previously reported that our hydrogel-based detection system is beneficial in performing multiplexed assays for small panels of miRNAs with a high level of specificity in a relatively short time period. In initial characterization, we compared the cellular miR-21 signals from singleplexed and multiplexed assays. There was no significant difference in miR-21 intensity between the two assays (Figure S2), demonstrating that our modified assay scheme is compatible with a multiplexed assay.

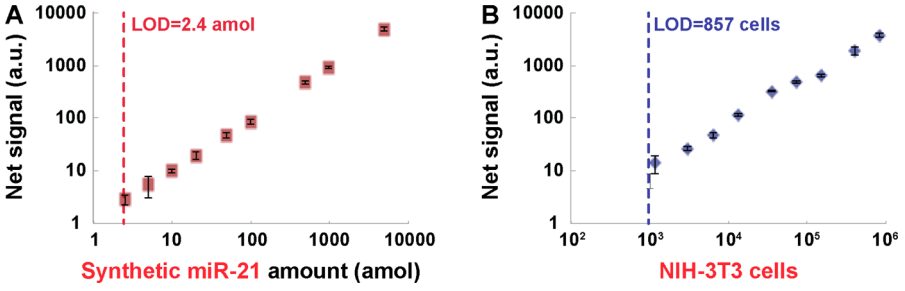

Figure 4. Calibration curves of (A) synthetic and (B) endogenous miR-21. The limit of detection was determined by fitting the points to a line and extrapolating to the point where the SNR was equal to 3. Error bars represent standard deviation (n = 4–8).

DOI: 10.1021/acs.analchem.5b03902
Anal. Chem. XXXX, XXX, XXX–XXX

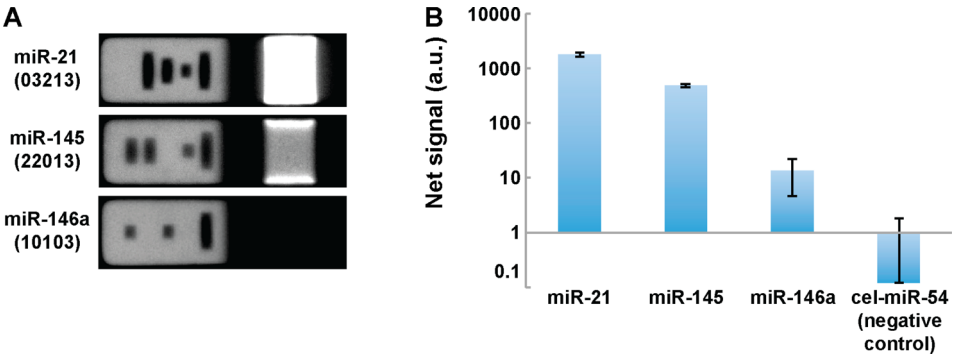

Figure 5. Multiplexed analysis. Graphically encoded particles with different miRNA probes were combined in the same reaction volume with NIH-3T3 cells. (A) A fluorescent image of a representative particle for each endogenous miRNA. (B) The net signal for each miRNA in the multiplex assay from 250 000 cells. Error bars represent one standard deviation (n = 4–9).

After characterization, we simultaneously measured three endogenous miRNA targets (miR-21, miR-145, miR-146a) from raw 3T3 cells by adding graphically encoded gel particles with different probes to the same reaction mixture. Their expression levels are known to be diverse in 3T3 cells, allowing us to demonstrate multiplexing abilities over a wide range of concentrations for diagnostically relevant targets. For multiplexing, all probe concentrations were rate matched as described in the Experimental Section and previous studies.[22,35] As illustrated in Figure 5, we observed dose-dependent signals from three endogenous targets. Specifically, the miR-145 signal is measured as ~0.27 relative to miR-21, which is well matched with previous Northern blot results (miR-145 signal was expected to be ~20% of miR-21 signal).[17] This correlation demonstrates the high efficiency of our lysis approach and high performance of our assay scheme. It is also important to note that there was no significant signal measured from particles containing probes for *C. elegans* miRNA (cel-miR-54), which is often used as a control (Figure 5A).[23,39,40] This result demonstrates the high reliability and specificity of our assay scheme.

CONCLUSIONS

In summary, we have developed a technique for direct measurement of unpurified cellular miRNA levels through the use of hydrogel particles and an optimized buffer for cell lysis and miRNA hybridization. Unlike previous studies, this assay demonstrates reliable measurement with small intratrial coefficients of variation (8–9%). Our graphically encoded barcode particles enabled multiplexed measurements for three endogenous miRNA targets (miR-21, miR-145, miR-146a). We also quantified the expression level of let-7a miRNA from raw HeLa cells (data not shown), indicating that our versatile assay scheme could potentially be extended to other cell types and miRNA targets. Moreover, in our highly flexible and scalable system, our current sensitivity (<1000 cells) can be improved, possibly to a single cell level, through incorporating signal-based amplification or running the assay in nanoliter chambers without the need for rigorous optimization. This single-cell assay would be beneficial in understanding cell-to-cell heterogeneity and characterizing rare cells.

ASSOCIATED CONTENT

Supporting Information

The Supporting Information is available free of charge on the ACS Publications website at DOI: 10.1021/acs.analchem.5b03902.

Additional supporting figures and tables are available as noted in text (PDF)

AUTHOR INFORMATION

Corresponding Author

*E-mail: pdoyle@mit.edu (P.S.D.).

Notes

The authors declare no competing financial interest.

ACKNOWLEDGMENTS

We acknowledge the support from the NIH-NCI Grant 5R21CA177393-02. We also thank David P. Bartel, Sean E. McGeary, and Joanna A. Stefano for providing 3T3 cells and useful discussions.

REFERENCES

(1) Calin, G. A.; Croce, C. M. *Nat. Rev. Cancer* **2006**, *6*, 857–866.
(2) Melo, S. A.; Esteller, M. *FEBS Lett.* **2011**, *585*, 2087–2099.
(3) Chen, P. S.; Su, J. L.; Hung, M. C. *J. Biomed. Sci.* **2012**, *19*, 90.
(4) Geaghan, M.; Cairns, M. J. *Biol. Psychiatry* **2015**, *78*, 231–239.
(5) Pandey, A. K.; Agarwal, P.; Kaur, K.; Datta, M. *Cell. Physiol. Biochem.* **2009**, *23*, 221–232.
(6) Small, E. M.; Olson, E. N. *Nature* **2011**, *469*, 336–342.
(7) Thum, T.; Mayr, M. *Cardiovasc. Res.* **2012**, *93*, 543–544.
(8) Pritchard, C. C.; Cheng, H. H.; Tewari, M. *Nat. Rev. Genet.* **2012**, *13*, 358–369.
(9) Chugh, P.; Dittmer, D. P. *Wiley interdisciplinary reviews. RNA* **2012**, *3*, 601–616.
(10) Baker, M. *Nat. Methods* **2010**, *7*, 687–692.
(11) Wang, B.; Howel, P.; Bruheim, S.; Ju, J.; Owen, L. B.; Fodstad, O.; Xi, Y. *PLoS One* **2011**, *6*, e17167.
(12) Mestdagh, P.; Hartmann, N.; Baeriswyl, L.; Andreasen, D.; Bernard, N.; Chen, C.; Cheo, D.; D'Andrade, P.; DeMayo, M.; Dennis, L.; Derveaux, S.; Feng, Y.; Fulmer-Smentek, S.; Gerstmayer, B.; Gouffon, J.; Grimley, C.; Lader, E.; Lee, K. Y.; Luo, S.; Mouritzen, P.; Narayanan, A.; Patel, S.; Peiffer, S.; Ruberg, S.; Schroth, G.; Schuster, D.; Shaffer, J. M.; Shelton, E. J.; Silveria, S.; Ulmanella, U.; Veeramachaneni, V.; Staedtler, F.; Peters, T.; Guettouche, T.; Wong, L.; Vandesompele, J. *Nat. Methods* **2014**, *11*, 809–815.
(13) Wang, H.; Ach, R. A.; Curry, B. *RNA* **2007**, *13*, 151–159.
(14) Nakayama, H.; Yamauchi, Y.; Taoka, M.; Isobe, T. *Anal. Chem.* **2015**, *87*, 2884–2891.

DOI: 10.1021/acs.analchem.5b03902
Anal. Chem. XXXX, XXX, XXX–XXX

(15) Yang, C.; Dou, B.; Shi, K.; Chai, Y.; Xiang, Y.; Yuan, R. *Anal. Chem.* **2014**, *86*, 11913−11918.
(16) Zhang, P.; Zhang, J.; Wang, C.; Liu, C.; Wang, H.; Li, Z. *Anal. Chem.* **2014**, *86*, 1076−1082.
(17) Rissland, O. S.; Hong, S. J.; Bartel, D. P. *Mol. Cell* **2011**, *43*, 993−1004.
(18) Shatzkes, K.; Teferedegne, B.; Murata, H. *Sci. Rep.* **2014**, *4*, 4659.
(19) Ho, Y. K.; Xu, W. T.; Too, H. P. *PLoS One* **2013**, *8*, e72463.
(20) Svec, D.; Andersson, D.; Pekny, M.; Sjoback, R.; Kubista, M.; Stahlberg, A. *Front. Oncol.* **2013**, *3*, 274.
(21) Ryoo, S. R.; Lee, J.; Yeo, J.; Na, H. K.; Kim, Y. K.; Jang, H.; Lee, J. H.; Han, S. W.; Lee, Y.; Kim, V. N.; Min, D. H. *ACS Nano* **2013**, *7*, 5882−5891.
(22) Chapin, S. C.; Appleyard, D. C.; Pregibon, D. C.; Doyle, P. S. *Angew. Chem., Int. Ed.* **2011**, *50*, 2289−2293.
(23) Chapin, S. C.; Doyle, P. S. *Anal. Chem.* **2011**, *83*, 7179−7185.
(24) Appleyard, D. C.; Chapin, S. C.; Doyle, P. S. *Anal. Chem.* **2011**, *83*, 193−199.
(25) Srinivas, R. L.; Chapin, S. C.; Doyle, P. S. *Anal. Chem.* **2011**, *83*, 9138−9145.
(26) Pregibon, D. C.; Doyle, P. S. *Anal. Chem.* **2009**, *81*, 4873−4881.
(27) Levicky, R.; Horgan, A. *Trends Biotechnol.* **2005**, *23*, 143−149.
(28) Sorokin, N. V.; Chechetkin, V. R.; Pan'kov, S. V.; Somova, O. G.; Livshits, M. A.; Donnikov, M. Y.; Turygin, A. Y.; Barsky, V. E.; Zasedatelev, A. S. *J. Biomol. Struct. Dyn.* **2006**, *24*, 57−66.
(29) Pregibon, D. C.; Toner, M.; Doyle, P. S. *Science* **2007**, *315*, 1393−1396.
(30) Dendukuri, D.; Gu, S. S.; Pregibon, D. C.; Hatton, T. A.; Doyle, P. S. *Lab Chip* **2007**, *7*, 818−828.
(31) Tang, F.; Hajkova, P.; Barton, S. C.; O'Carroll, D.; Lee, C.; Lao, K.; Surani, M. A. *Nat. Protoc.* **2006**, *1*, 1154−1159.
(32) Petriv, O. I.; Kuchenbauer, F.; Delaney, A. D.; Lecault, V.; White, A.; Kent, D.; Marmolejo, L.; Heuser, M.; Berg, T.; Copley, M.; Ruschmann, J.; Sekulovic, S.; Benz, C.; Kuroda, E.; Ho, V.; Antignano, F.; Halim, T.; Giambra, V.; Krystal, G.; Takei, C. J.; Weng, A. P.; Piret, J.; Eaves, C.; Marra, M. A.; Humphries, R. K.; Hansen, C. L. *Proc. Natl. Acad. Sci. U. S. A.* **2010**, *107*, 15443−15448.
(33) Choi, N. W.; Kim, J.; Chapin, S. C.; Duong, T.; Donohue, E.; Pandey, P.; Broom, W.; Hill, W. A.; Doyle, P. S. *Anal. Chem.* **2012**, *84*, 9370−9378.
(34) Srinivas, R. L.; Johnson, S. D.; Doyle, P. S. *Anal. Chem.* **2013**, *85*, 12099−12107.
(35) Lee, H.; Srinivas, R. L.; Gupta, A.; Doyle, P. S. *Angew. Chem., Int. Ed.* **2015**, *54*, 2477−2481.
(36) Schneider, C. A.; Rasband, W. S.; Eliceiri, K. W. *Nat. Methods* **2012**, *9*, 671−675.
(37) Brown, R. B.; Audet, J. *J. R. Soc., Interface* **2008**, *5* (S2), S131−138.
(38) Hilz, H.; Wiegers, U.; Adamietz, P. *Eur. J. Biochem.* **1975**, *56*, 103−108.
(39) Arroyo, J. D.; Chevillet, J. R.; Kroh, E. M.; Ruf, I. K.; Pritchard, C. C.; Gibson, D. F.; Mitchell, P. S.; Bennett, C. F.; Pogosova-Agadjanyan, E. L.; Stirewalt, D. L.; Tait, J. F.; Tewari, M. *Proc. Natl. Acad. Sci. U. S. A.* **2011**, *108*, 5003−5008.
(40) Li, Y.; Kowdley, K. V. *Anal. Biochem.* **2012**, *431*, 69−75.

DOI: 10.1021/acs.analchem.5b03902
Anal. Chem. XXXX, XXX, XXX−XXX